THE JOURNAL OF PHYSICAL CHEMISTRY Letters

Cite This: J. Phys. Chem. Lett. 2018, 9, 3703−3707

Letter

pubs.acs.org/JPCL

Modeling the Role of Excluded Volume in Zeolite Structure Direction

Cecilia Bores,[†] Scott M. Auerbach,*[,‡] and Peter A. Monson*[,†]

[†]Department of Chemical Engineering and [‡]Department of Chemistry, University of Massachusetts Amherst, Amherst, Massachusetts 01003, United States

Supporting Information

ABSTRACT: We investigate the formation of zeolite structures in replica-exchange Monte Carlo simulations of a reactive model of silica polymerization. The simulations incorporate hard spheres to model the effect of excluded volume caused by structure-directing agents (SDAs). We focus on modeling the formation of cage-type zeolite frameworks SOD and LTA. Our model predicts that a relatively wide range of SDA sizes could be used to construct SOD, whereas a narrower range will work for constructing LTA. We also predict that there is potential benefit of including multiple SDAs in each zeolite unit cell, and in the case of LTA with both small and large cavities, there is a strong potential benefit using both small and large SDAs that match the cavities' sizes. We hypothesize that the volume exclusion reduces the configuration space available to the assembling silica units, making it easier for the system to find ordered structures with quasi-spherical cavities.

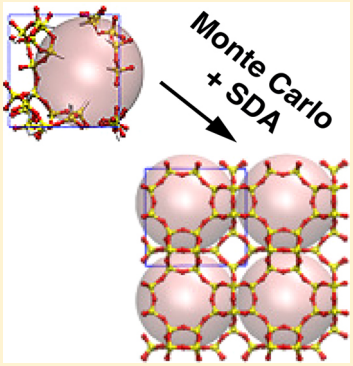

Zeolites are one of the most important nanoporous materials due to their regular and stable arrays of connected nanopores. Tailoring and controlling the size and shape of zeolite nanopores is of paramount importance for specific applications such as reactions of bulky feedstocks, shape-selective catalysis, and separations.[1] Such targeted zeolite syntheses would be facilitated by a deeper understanding of zeolite formation processes, the effects of synthesis conditions over the resulting zeolite phase,[2−5] and the roles of structure directing agents (SDAs). Several studies on zeolite formation have been reported including reviews that correlate the nature of SDAs with resulting zeolites,[2−5] studies that measure thermodynamic heats of adsorption of SDAs during zeolite synthesis,[6] and studies that compute synthesizable SDAs for known, target zeolites.[7] SDAs are thought to stabilize pores and channels in precursor silica networks via a range of interactions including electrostatic charge balancing with anionic silicates, hydrophobic attractions to silica,[8] and van der Waals interactions.[9] However, it is not clear which, if any, of these interactions may dominate during zeolite structure formation. In this Letter, we report on reactive ensemble Monte Carlo simulations, revealing that the volume−exclusion interaction alone can facilitate zeolite crystal formation.

Identifying atomic-level structures that lead to zeolite crystals remains challenging for characterization methods due to their "nanoscale blindspot" around length scales key for zeolite nucleation (5−10 nm).[10] To address this, a broad range of molecular simulations have offered insights into zeolite formation.[11] Here we apply a previously published, coarse-grained model of silica polymerization (represented in Figure 1 and fully described in Supporting Information Section S1)[12−14] sampled with an enhanced replica-exchange reactive

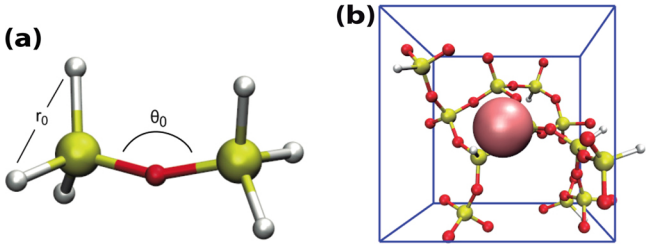

Figure 1. (a) Silica tetrahedral model. Silicon atoms are represented in yellow and oxygenic species in white (if terminal hydroxyls) or in red (if bridging oxygens). Tetrahedral shape and flexibility are ensured by O−O intratetrahedron and Si−O−Si intertetrahedral angular springs. (b) Silica tetrahedra polymerizing in the presence of an SDA particle.

Monte Carlo (RE-RxMC) method capable of simulating the formation of zeolite crystals.[15,16] RE-RxMC speeds up equilibration by simultaneously simulating several system copies, each with a different value of the equilibrium constant controlling silica hydrolysis.[17] Primitive RE-RxMC sampling of our silica model was found to construct crystals for ATT, DFT, EDI, and SOD zeolites,[15] all frameworks with relatively small unit cells—no larger than 12 tetrahedra.[18] Replica-exchange methods often run into problems modeling first-order phase transitions because of the presence of free-energy barriers between phases. Using an adaptive grid that concentrates replicas in the barrier region has been found to mitigate this

Received: May 9, 2018
Accepted: June 16, 2018
Published: June 16, 2018

DOI: 10.1021/acs.jpclett.8b01467
J. Phys. Chem. Lett. 2018, 9, 3703−3707

problem.[19−21] Thus extending the RE-RxMC approach to larger zeolite unit cells was accomplished by implementing an adaptive grid of equilibrium constant values.[16] (A comprehensive description of the method and parameters is given in Supporting Information Figure S1 and Table S1.) We found optimal results by targeting for a Gaussian exchange−probability profile in the region of replicas where the exchange probability would otherwise plummet, allowing the simulated construction of the AWW alumino-phosphate framework with 24 silica tetrahedra per unit cell.[16] However, this same approach failed to simulate the construction of the LTA zeolite framework, which also contains 24 silica tetrahedra per unit cell. This raises the central question of the present work—why did the adaptive RE-RxMC approach succeed for AWW and fail for LTA when their unit cells are the same size?

We suspect that framework density is key to answering this question. The framework density of zeolite LTA is 14.2 tetrahedral (T = Si or other tetrahedrally coordinated atoms such as Al) atoms per 1000 Å^3, while that for AWW zeolite is 16.9 T atoms per 1000 Å^3,[18] 19% higher than that for LTA. As a result, the largest sphere that fits in LTA is ∼11 Å in diameter, while that for AWW is only 7.5 Å. We thus hypothesize that RE-RxMC finds it challenging to construct a crystal of LTA's large-pore structure, and that adding an SDA into an RE-RxMC simulation of LTA formation will increase the effective total system density and facilitate LTA crystallization. In the present work, we introduce space-filling (i.e., hard sphere) SDAs to determine what effect, if any, they may have on zeolite formation, and find in the context of LTA zeolite topology that hard-sphere SDAs can play an essential role in promoting the formation of zeolite crystals.

In considering how to build our base-case model of SDA−silica and SDA−SDA interactions, we note that the success of our spring-tetrahedron/RxMC method stems from including only the essential chemistry and physics to keep the computations sufficiently simple to reach zeolite crystal formation. Consistent with this spirit and with the philosophy of Davis and coworkers,[22,23] we posit that SDA size and shape are the base-case properties that influence zeolite pore formation. For simplicity, we model these properties via volume exclusion with hard-sphere SDA−silica and SDA−SDA interactions. SDA hard spheres interact with silica tetrahedra in our model via hard spheres located on silicon atoms. In general, all hard-sphere interactions in our model satisfy the Lorentz combination rule: $\sigma_{ij} = (\sigma_i + \sigma_j)/2$, where i and j vary over Si, SDA1, and SDA2 (in the case of different SDAs). We note that oxygens in our silica model do not exclude volume for computational simplicity. As a result, the effective volume occupied by an SDA with diameter σ_{SDA} is somewhat less than the naïve value given by $\frac{4\pi}{3}(\sigma_{SDA}/2)^3$ because SDA−oxygen overlaps are allowed in our present simulations. In particular, in the case of a collinear Si−O−SDA geometry, an SDA in our model acts as if its diameter is $\sigma_{SDA} - 1.2$ Å, where 1.2 Å is the effective diameter of oxygen in our model. All hard-sphere and spring interactions satisfy periodic boundary conditions in our simulations.

SOD, LTA, and FAU zeolites are all constructed by connecting sodalite cages in different ways (as shown in Figure 2) and can all be synthesized with tetra-methylammonium (TMA) as the SDA.[24−26] The SOD unit cell contains two sodalite cages, each of which can fit a sphere no larger than 6.3 Å in diameter, whereas LTA has two cavity sizes: a small

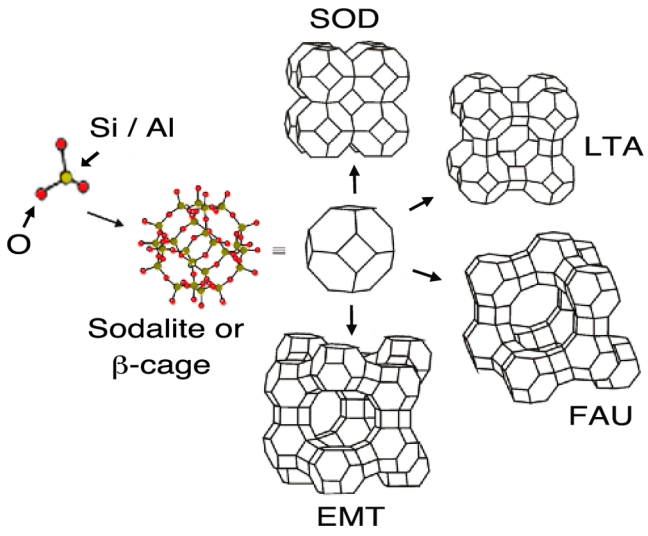

Figure 2. Hierarchical structure of zeolites SOD, LTA, FAU, and EMT, all of them based on sodalite cage. Adapted from Newsam.[27]

cavity given by the sodalite cage and a larger cavity (the so-called "α" cage[27]) that can accommodate a sphere no larger than 11.1 Å in diameter. In principle, these two length scales determine the sizes of hard spheres that can act as successful SDAs for SOD and LTA crystallization. In the present work, we model SDA as a single hard sphere, and we vary its hard-sphere radius to determine how SDA size can influence crystallization. We study SOD below to compare RE-RxMC crystallization results without an SDA[15,16] to results with SDA(s). We study LTA to determine if reducing free volume can facilitate crystal construction in RE-RxMC. Figures S2 and S3 in the Supporting Information show the XRD patterns of the crystal structures we have found for SOD and LTA, respectively, in comparison with those structures given by IZA database.[18] We find below that SDA volume exclusion can facilitate zeolite formation, and for LTA, SDAs with different sizes can dramatically speed crystallization.

We begin by showing results for RE-RxMC simulations of SOD crystallization with no SDA, one SDA, and two identical SDAs per unit cell in Figure 3a,b. Snapshots illustrating those situations can be found in Supporting Information Figure S4. The y axes in these Figures show the degree of polymerization, which starts at zero before any silica condensation has occurred and can grow to a value of unity for a fully connected, crystalline silica network. The results shown in Figure 3a,b correspond to the replica with the largest equilibrium constant for silica condensation, which drives silica network formation and thus crystallization, and are averaged over the 20 independent RE-RxMC runs. Figure 3a shows results for SOD with SDAs ranging in size from σ_{SDA} = 4.0 to 8.0 Å for comparison with RE-RxMC simulations with no SDA. The number of crystals found for each case and results from additional combinations of SDA sizes are shown in Supporting Information Table S2. The results for no SDA and for one SDA (up to 7.0 Å) show crystallization; the reason that the average degree of polymerization does not reach unity is that most, but not all, replicas in the simulations form crystals.

The results in Figure 3a show that including an SDA has no effect on SOD crystallization in our RE-RxMC simulations, as long as the SDA is not too large. Indeed, excluding the case of one SDA (σ_{SDA} = 8.0 Å), all of the results in Figure 3a show

DOI: 10.1021/acs.jpclett.8b01467
J. Phys. Chem. Lett. 2018, 9, 3703−3707

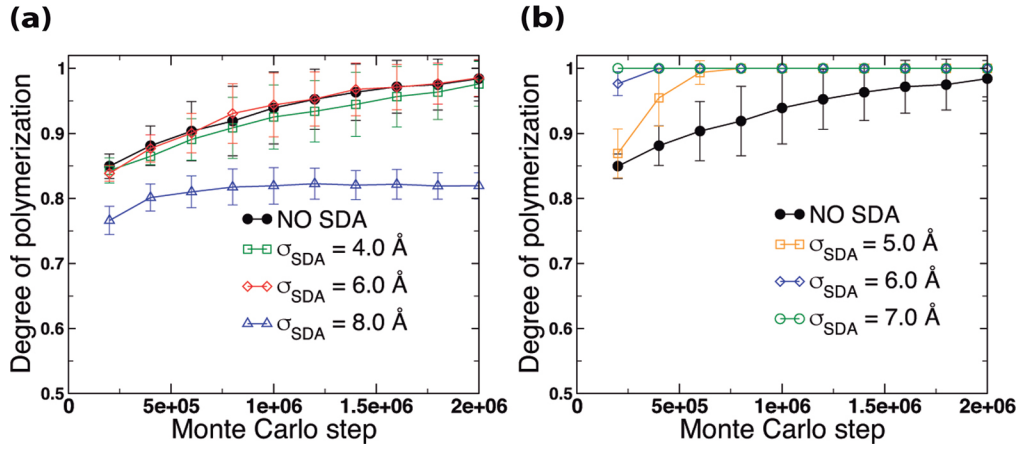

Figure 3. Evolution of the degree of polymerization as a function of the number of RE-RxMC steps for zeolite SOD averaged over 20 independent runs. (a) 1 SDA: Including one SDA has little effect if the SDA is not too large. (b) 2 SDAs: Including two SDAs can dramatically speed up crystallization. Overall, most simulations make SOD crystals.

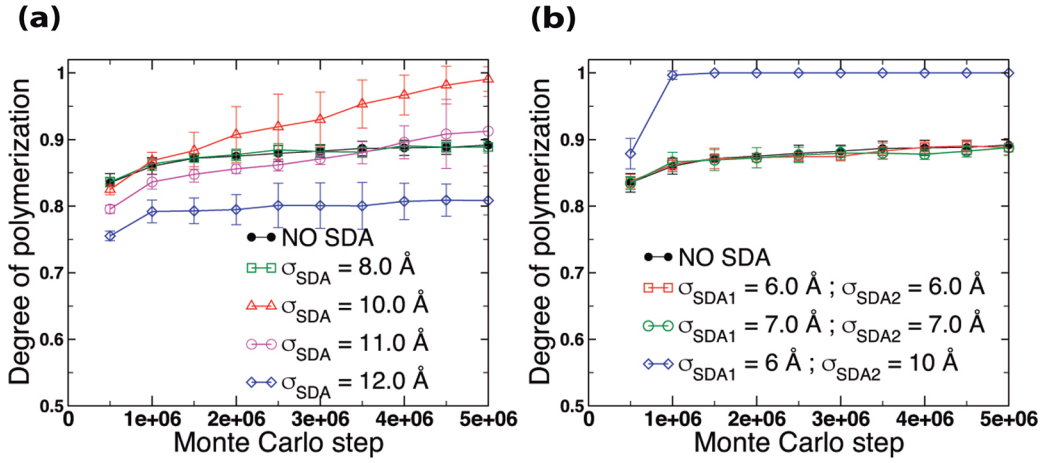

Figure 4. Evolution of the degree of polymerization as a function of the number of RE-RxMC steps for zeolite LTA averaged over five independent runs. (a) 1 SDA: predicts an optimal size (10.0 Å); (b) 2 SDAs: predicts a combination of SDA sizes (6.0, 10.0 Å) that promotes crystallization. Overall, relatively few simulations make LTA crystals.

essentially the same rate of change of the degree of polymerization with the number of Monte Carlo steps, with roughly the same statistics among the 20 statistically independent simulations. However, including an SDA with σ_{SDA} = 8.0 Å clearly arrests crystallization, forcing the degree of polymerization in the constant volume simulation cell to saturate at ∼0.82. This result makes sense given that the SOD cage, acting like one with σ_{SDA} = 6.8 Å cannot fit a sphere larger than 6.3 Å in diameter. Thus not only does using a large SDA impede SOD crystallization but also it hampers silica polymerization because of the limited space available in our fixed-volume simulations.

Figure 3b reveals a substantially different situation, showing the results of RE-RxMC simulations of SOD crystallization with two identical SDAs for comparison with the case of no SDA (black line). Figure 3b shows that including two SDAs dramatically changes both the rate and statistics of SOD crystallization, especially when the SDA size approaches the SOD cage size. As a point of comparison, we see in Figure 3b that using no SDA (black line) requires about 1 million Monte Carlo steps to produce SOD crystals. In contrast, using two SDAs with σ_{SDA} = 6.0 Å (blue line) causes all replicas to form SOD crystals by ∼0.4 million Monte Carlo steps. Furthermore, using two SDAs with σ_{SDA} = 7.0 Å (green line) causes all replicas to form SOD crystals by ∼0.05 million Monte Carlo steps. We note that because of allowed SDA−oxygen overlaps in our model, an SDA with σ_{SDA} = 7.0 Å acts like one with σ_{SDA} = 5.8 Å, which can well fit into the sodalite cage. The results on SOD in Figure 3b suggest that tuning the concentration of SDAs in zeolite synthesis can impact the rate and likelihood of forming crystals.

Figure 4a,b show results for RE-RxMC simulations of LTA crystallization with no SDA, one SDA, two identical SDAs, and two different SDAs per unit cell as a function of SDA size over the range 8.0−12.0 Å. Snapshots illustrating those situations can be found in Supporting Information Figure S5. The number of crystals found for each case and results from additional combinations of SDA sizes are shown in Supporting Information Table S3. *Y* axes in Figure 4a,b show the same quantity as in Figure 3; in the case of Figure 4, the degree of polymerization corresponds to the replica with the largest equilibrium constant for silica condensation and is averaged over five independent RE-RxMC runs. Figure 4a shows a very different result from that in Figure 3a. In the SOD case with zero or one SDA (Figure 3a), nearly all of the runs produced SOD crystals, except when the SDA could not fit in the SOD

DOI: 10.1021/acs.jpclett.8b01467
J. Phys. Chem. Lett. 2018, 9, 3703−3707

cage. For LTA with zero or one SDA (Figure 4a), most of the runs do not produce LTA crystals. In the case of one SDA with σ_{SDA} = 10.0 Å (red line), we observe LTA crystal formation in four out of five independent simulations after ∼3.5 million steps, whereas one SDA with σ_{SDA} = 11.0 Å (pink line) gives LTA crystals in only one out of five simulations after 3.9 million steps. No other RE-RxMC simulation on the LTA unit cell with one SDA produced crystals.

We note that LTA can be synthesized experimentally with TMA as the SDA, which features a diameter close to 6 Å.[28] Upon first consideration, this may seem discrepant with our prediction of 10 Å as the optimal SDA size. However, we also note that LTA zeolites made with TMA are typically aluminosilicates with relatively high alumina content and hence low silica content. Synthesizing all-silica or even high-silica LTA (Si:Al > 3) with an SDA as small as TMA has remained very challenging. Corma and coworkers reported the synthesis of high-silica LTA using SDAs that engage in supramolecular $\pi-\pi$ stacking inside the LTA α-cage.[29] Whereas such SDA dimers are clearly quite different from hard spheres, our predicted length scale of 10 Å is certainly consistent with an effective diameter of Corma's supramolecular SDA dimer.

Using too large an SDA (12.0 Å, blue line) prevents crystallization and perturbs silica polymerization by a statistically significant extent, reducing the plateau value of the degree of polymerization from ∼0.9 to just over 0.8. Overall, Figure 4a predicts an optimal SDA size (10.0 Å, red line) for producing LTA crystals in our model with one SDA per unit cell.

Figure 4b shows results for LTA comparing no SDA, two identical SDAs of sizes 6.0 to 7.0 Å, and one case of two different SDAs with sizes 6.0 and 10.0 Å. The striking prediction in Figure 4b is that crystallization of LTA can be promoted by using SDAs with sizes that match the pore sizes of the sodalite and α-cages (6.0 and 10.0 Å, respectively). In this case, LTA crystallization was found to take place after only 1 million steps, nearly four times faster (in Monte Carlo steps) than that observed for LTA with one SDA. In a forthcoming publication, we will report on more such simulations of zeolite crystallization for frameworks with multiple pore sizes and with SDAs of matching or mismatching sizes.

In conclusion, we have developed a model to examine the role of SDA volume exclusion in the construction of zeolite frameworks, with a focus on the SOD and LTA zeolite structures. When sampled with replica-exchange reaction ensemble Monte Carlo (Re-RxMC), our model predicts that a relatively wide range of SDA sizes could be used to construct SOD, while a narrower range will work for constructing LTA. We also predict that there is potential benefit of including multiple SDAs in each zeolite unit cell, and in the case of LTA with both small and larger cavities, there is a strong potential benefit using both small and large SDAs that match the cavities' sizes. While our model is necessarily simple—to be able to reach the effective time scales associated with zeolite crystal formation—our model has yielded plausible and testable predictions (especially for cage-type zeolites) that can move forward the field of rational zeolite synthesis.

The mechanism by which volume exclusion promotes crystalline order in our simulations is quite straightforward. A spherical excluded volume in our simulations narrows the accessible configuration space for the polymerizing silica units to regions more closely resembling those occupied by the crystalline silica in sodalite units. This comports with quite primitive notions of templating and structure direction.

METHODS

In general, the RE-RxMC simulations reported here were performed in the same manner as in our previous publication.[16] except with the present addition of SDAs; for completeness, we offer key simulation details. All simulations were performed at constant volume; in a forthcoming publication we will report the results of constant pressure RE-RxMC simulations, allowing the volume to fluctuate. Simulation cells and initial configurations were constructed as described in the Supporting Information Section S1. Monte Carlo moves of silica tetrahedra were performed as we have previously described,[13,14] and Monte Carlo moves of SDAs were performed with standard, unbiased displacements. All parameters describing these displacements are given in Supporting Information Table S1.

RE-RxMC simulations were performed in parallel to the number of replicas and with temperature fixed. The number of replicas was typically 16 for simulations of SOD and 28 for LTA, while the temperature was fixed at 300 K. Although heating the system may enable crystallization, as occurs in experimental zeolite syntheses, we used the adaptive RE-RxMC grid to facilitate zeolite formation. The adaptive grid of hydrolysis equilibrium constants was initialized and updated as in our previous work, with a target Gaussian exchange probability profile centered on the regime of replicas spanning a free-energy barrier separating amorphous and crystalline phases. The required RE-RxMC simulation length was found to depend on the system under study: 2 million steps was sufficient for constructing SOD crystals, while 5 million steps were required for LTA. To further increase the likelihood of forming SOD and LTA crystals, several runs of RE-RxMC were performed with thermodynamically identical but statistically independent initial conditions; this number of identical RE-RxMC runs (N_{runs}) was typically set to 20 for SOD and 5 for LTA simulations. In principle, running longer simulations, including more replicas, and running more independent copies could change our observed results in terms of the systems that do and do not form zeolite crystals. We have fixed the simulation run time and the number of independent copies to the values given above as a benchmark to determine the efficiency of the method to find crystal structures.

ASSOCIATED CONTENT

Supporting Information

The Supporting Information is available free of charge on the ACS Publications website at DOI: 10.1021/acs.jpclett.8b01467.

Comprehensive description of the reactive model of silica polymerization and RE-RxMC method, protocol, and parameters used in this work; complete set of results for the SOD and LTA crystal finding efficiency of the simulations; and zeolite structural information: XRD and snapshots. (PDF)

AUTHOR INFORMATION

Corresponding Authors

*E-mail: auerbach@chem.umass.edu. Tel: +1 413-545-1240.
*E-mail: monson@ecs.umass.edu. Tel: +1 413-545-0661.

ORCID

Cecilia Bores: 0000-0002-7359-1556

DOI: 10.1021/acs.jpclett.8b01467
J. Phys. Chem. Lett. 2018, 9, 3703−3707

Notes

The authors declare no competing financial interest.

■ ACKNOWLEDGMENTS

This work was supported by the U.S. Department of Energy (contract no. DE-FG02-07ER46466). We are grateful for computational resources provided by the Massachusetts Green High-Performance Computing Center (MGHPCC). We also acknowledge Dr. S. Chien for assistance with the Monte Carlo code.

■ REFERENCES

(1) Auerbach, S. M.; Karrado, K. A.; Dutta, P. K. *Handbook of Zeolite Science and Technology*; Marcel Dekker: New York, 2003.
(2) Lobo, R. F.; Zones, S. I.; Davis, M. E. Structure-Direction in Zeolite Synthesis. *J. Inclusion Phenom. Mol. Recognit. Chem.* **1995**, *21*, 47−78.
(3) Cundy, C. S.; Cox, P. A. The Hydrothermal Synthesis of Zeolites: Precursors, Intermediates and Reaction Mechanism. *Microporous Mesoporous Mater.* **2005**, *82*, 1−78.
(4) Jiang, J.; Yu, J. H.; Corma, A. Extra-Large-Pore Zeolites: Bridging the Gap between Micro and Mesoporous Structures. *Angew. Chem., Int. Ed.* **2010**, *49*, 3120−3145.
(5) Zones, S. I. Translating New Materials Discoveries in Zeolite Research to Commercial Manufacture. *Microporous Mesoporous Mater.* **2011**, *144*, 1−8.
(6) Piccione, P. M.; Yang, S.; Navrotsky, A.; Davis, M. E. Thermodynamics of Pure-Silica Molecular Sieve Synthesis. *J. Phys. Chem. B* **2002**, *106*, 3629−3638.
(7) Pophale, R.; Daeyaert, F.; Deem, M. W. Computational Prediction of Chemically Synthesizable Organic Structure Directing Agents for Zeolites. *J. Mater. Chem. A* **2013**, *1*, 6750−6760.
(8) Burkett, S. L.; Davis, M. E. Mechanisms of Structure Direction in the Synthesis of Pure-Silica Zeolites. 1. Synthesis of TPA/Si-SZM-5. *Chem. Mater.* **1995**, *7*, 920−928.
(9) Burton, A. W.; Lee, G. S.; Zones, S. I. Phase Selectivity in the Syntheses of Cage-Based Zeolite Structures: an Investigation of Thermodynamic Interactions Between Zeolite Hosts and Structure Directing Agents by Molecular Modeling. *Microporous Mesoporous Mater.* **2006**, *90*, 129−144.
(10) Davis, T. M.; Drews, T. O.; Ramanan, H.; He, C.; Dong, J.; Schnablegger, H.; Katsoulakis, M. A.; Kokkoli, E.; McCormick, A. V.; Penn, R. L.; et al. Mechanistic Principles of Nanoparticle Evolution of Zeolite Crystals. *Nat. Mater.* **2006**, *5*, 400−408.
(11) Auerbach, S. M.; Fan, W.; Monson, P. A. Modelling the assembly of nanoporous silica materials. *Int. Rev. Phys. Chem.* **2015**, *34*, 35−70.
(12) Astala, R.; Auerbach, S. M.; Monson, P. A. Normal Mode Approach for Predicting the Mechanical Properties of Solids from First Principles: Application to Compressibility and Thermal Expansion of Zeolites. *Phys. Rev. B: Condens. Matter Mater. Phys.* **2005**, *71*, 014112.
(13) Malani, A.; Auerbach, S. M.; Monson, P. A. Probing the Mechanism of Silica Polymerization at Ambient Temperatures using Monte Carlo Simulations. *J. Phys. Chem. Lett.* **2010**, *1*, 3219−3224.
(14) Malani, A.; Auerbach, S. M.; Monson, P. A. Monte Carlo Simulations of Silica polymerisation and Network Formation. *J. Phys. Chem. C* **2011**, *115*, 15988−16000.
(15) Chien, S.-C.; Auerbach, S. M.; Monson, P. A. Reactive Ensemble Monte Carlo Simulations of Silica Polymerization That Yield Zeolites and Related Crystalline Microporous Structures. *J. Phys. Chem. C* **2015**, *119*, 26628−26635.
(16) Bores, C.; Auerbach, S. M.; Monson, P. A. Enhanced Replica Exchange Reactive Monte Carlo Simulations for Constructing Zeolite Frameworks. *Mol. Simul.* **2018**, *44*, 453−462.
(17) Turner, C.; Brennan, J.; Lisal, M. Replica Exchange for Reactive Monte Carlo Simulations. *J. Phys. Chem. C* **2007**, *111*, 15706−15715.
(18) Baerlocher, C.; McCusker, L. B.; Olson, D. *Atlas of Zeolite Framework Types*, 6th ed.; Elsevier: Amsterdam, 2007.
(19) Predescu, C.; Predescu, M.; Ciobanu, C. V. On the Efficiency of Exchange in Parallel tempering Monte Carlo simulations. *J. Phys. Chem. B* **2005**, *109*, 4189−4196.
(20) Katzgraber, H.; Trebst, S.; Huse, D.; Troyer, M. Feedback-Optimized Parallel Tempering Monte Carlo. *J. Stat. Mech.: Theory Exp.* **2006**, *2006*, P03018.
(21) Trebst, S.; Troyer, M.; Hansmann, U. Optimized Parallel Tempering Simulations of Proteins. *J. Chem. Phys.* **2006**, *124*, 174903.
(22) Davis, M. E.; Lobo, R. F. Zeolite and Molecular Sieve Synthesis. *Chem. Mater.* **1992**, *4*, 756−768.
(23) Davis, M. E. Zeolites from a Materials Chemistry Perspective. *Chem. Mater.* **2014**, *26*, 239−245.
(24) Baerlocher, H.; Meier, W. M. Synthese und Kristallstruktur von Tetramethylammonium-Sodalith. *Helv. Chim. Acta* **1969**, *52*, 1853−1860.
(25) Mintova, S.; Olson, N.; Bein, T. Electron Microscopy Reveals the Nucleation Mechanism of Zeolite Y from Precursor Colloids. *Angew. Chem., Int. Ed.* **1999**, *38*, 3201−3204.
(26) Fan, W.; Shirato, S.; Gao, F.; Ogura, M.; Okubo, T. Phase selection of FAU and LTA Zeolites by Controlling Synthesis Parameters. *Microporous Mesoporous Mater.* **2006**, *89*, 227−234.
(27) Newsam, J. M. The Zeolite Cage Structure. *Science* **1986**, *231*, 1093−1099.
(28) Aue, D. H.; Webb, H. M.; Bowers, M. T. A Thermodynamic Analysis of Solvation Effects on the Basicites of Alkylamines. An Electrostatic Analysis of Substituents Effects. *J. Am. Chem. Soc.* **1976**, *98*, 318−329.
(29) Corma, A.; Rey, F.; Rius, J.; Sabater, M. J.; Valencia, S. Supramolecular self-assembled molecules as organic directing agent for synthesis of zeolites. *Nature* **2004**, *431*, 287−290.

DOI: 10.1021/acs.jpclett.8b01467
J. Phys. Chem. Lett. 2018, 9, 3703−3707